AD-A108 175   FOREIGN TECHNOLOGY DIV WRIGHT-PATTERSON AFB OH   F/G 20/14
ANTENNA (SELECTED ARTICLES),(U)
NOV 81 O G VENDIK, L V RIZHKOVA
UNCLASSIFIED   FTD-ID(RS)T-1134-81   NL

END
DATE
FILMED
82
DTIC

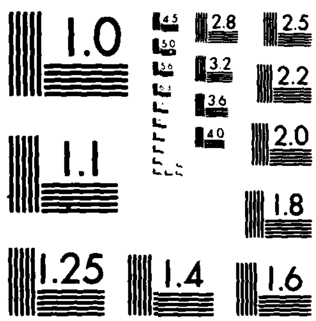

MICROCOPY RESOLUTION TEST CHART

NATIONAL BUREAU OF STANDARDS-1963-A

FTD-ID(RS)T-1134-81

FOREIGN TECHNOLOGY DIVISION

AIR FORCE SYSTEMS COMMAND

ANTENNA
(Selected Articles)

FOREIGN TECHNOLOGY DIVISION

Approved for public release;
distribution unlimited.

EDITED TRANSLATION

FTD-ID(RS)T-1134-81 6 November 1981

MICROFICHE NR: FTD-81-C-001012

ANTENNA (Selected Articles)

English pages: 27

Source: Antenny, Nr. 10, 1971, pp. 3-26

Country of origin: USSR
Translated by: Victor Mesenzeff
Requester: FTD/TQFE

THIS TRANSLATION IS A RENDITION OF THE ORIGINAL FOREIGN TEXT WITHOUT ANY ANALYTICAL OR EDITORIAL COMMENT. STATEMENTS OR THEORIES ADVOCATED OR IMPLIED ARE THOSE OF THE SOURCE AND DO NOT NECESSARILY REFLECT THE POSITION OR OPINION OF THE FOREIGN TECHNOLOGY DIVISION.	PREPARED BY: TRANSLATION DIVISION FOREIGN TECHNOLOGY DIVISION WP-AFB, OHIO.

14160 5/

TABLE OF CONTENTS

U. S. BOARD ON GEOGRAPHIC NAMES TRANSLITERATION SYSTEM

Block	Italic	Transliteration	Block	Italic	Transliteration
А а	*А а*	A, a	Р р	*Р р*	R, r
Б б	*Б б*	B, b	С с	*С с*	S, s
В в	*В в*	V, v	Т т	*Т т*	T, t
Г г	*Г г*	G, g	У у	*У у*	U, u
Д д	*Д д*	D, d	Ф ф	*Ф ф*	F, f
Е е	*Е е*	Ye, ye; E, e*	Х х	*Х х*	Kh, kh
Ж ж	*Ж ж*	Zh, zh	Ц ц	*Ц ц*	Ts, ts
З з	*З з*	Z, z	Ч ч	*Ч ч*	Ch, ch
И и	*И и*	I, i	Ш ш	*Ш ш*	Sh, sh
Й й	*Й й*	Y, y	Щ щ	*Щ щ*	Shch, shch
К к	*К к*	K, k	Ъ ъ	*Ъ ъ*	"
Л л	*Л л*	L, l	Ы ы	*Ы ы*	Y, y
М м	*М м*	M, m	Ь ь	*Ь ь*	'
Н н	*Н н*	N, n	Э э	*Э э*	E, e
О о	*О о*	O, o	Ю ю	*Ю ю*	Yu, yu
П п	*П п*	P, p	Я я	*Я я*	Ya, ya

*ye initially, after vowels, and after ъ, ь; e elsewhere.
When written as ё in Russian, transliterate as yё or ё.

RUSSIAN AND ENGLISH TRIGONOMETRIC FUNCTIONS

Russian	English	Russian	English	Russian	English
sin	sin	sh	sinh	arc sh	$\sinh^{-1}$
cos	cos	ch	cosh	arc ch	$\cosh^{-1}$
tg	tan	th	tanh	arc th	$\tanh^{-1}$
ctg	cot	cth	coth	arc cth	$\coth^{-1}$
sec	sec	sch	sech	arc sch	sech^{-1}
cosec	csc	csch	csch	arc csch	csch^{-1}

Russian	English
rot	curl
lg	log

COORDINATION OF A LINEAR PHASED ARRAY
OF WAVEGUIDE RADIATORS WITH WIDE-ANGLE
SCANNING IN THE E PLANE

O. G. Vendik and L. V. Rizhkova

This work examines a system of linear antenna array of waveguide radiators which permits the compensation of the variation in the reflection coefficient at the input of the system in the scanning sector. The parameters of the system were determined. The calculation carried out for the dependence of the reflection coefficient at the input on the scanning angle shows that the compensation improves the coordination significantly in a wide scan sector.

Formulation of the Problem

The problem of matching a phased array in a wide scanning sector arises as a result of the fact that when the position of the beam changes the fields induced due to the interrelationship between the elements also change; consequently, the modulus and phase of the reflection coefficient change in each channel.

The object of this work is to investigate the possibilities of minimizing of the reflection coefficient at the input of an arbitrary element of a linear array of waveguide radiators over a wide scan sector. This waveguide scheme for the excitation of the array is a development of the connecting-circuit technique proposed by Hannan [1] and discussed by the authors in [2, 3, and 4].

Let us examine the construction of Fig. 1. Here, regions I and III are waveguide arrays with cross section ab, whose wide sides are adjacent to one another. Regions II and IV are systems of parallel plates

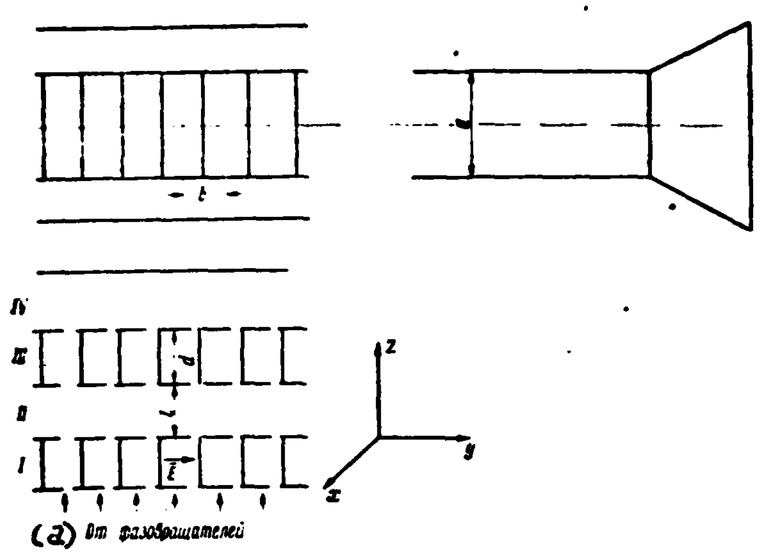

KEY: (a) From phase shifters

Fig. 1.

with the distance between them equalling a. If all the waveguides are excited inphase, the plane wave travels from one region to the other without distortions, and the reflection coefficient in any section of region I is equal to zero. When an array with a progressive phase shift is excited, a reflected wave appears at the input of the system. It is necessary to select the electrical lengths of regions II and III such that the reflection coefficient at the input of the system will remain relatively small, when scanning over a wide sector.

Determining the field structure in region II

Basic-type field in region I:

$$\left.\begin{aligned} {}_I E_y &= E_0 \cos\frac{\pi x}{a}\, e^{i m_y \psi_0}\left(e^{-i\gamma z} + R_1 e^{i\gamma z}\right) \\ {}_I H_x &= -\frac{\gamma}{\omega\mu_0} E_0 \cos\frac{\pi x}{a}\, e^{i m_y \psi_0}\left(e^{-i\gamma z} - R_1 e^{i\gamma z}\right) \end{aligned}\right\},$$

where $m_{(y)}\psi_0$ is a phase shift between waveguides due to the control system; R_1 - coefficient of reflection from the boundary I–II for the basic type.

The field of incident waves in region II we write in the form of the Fourier-integral expansion in the k derivative of y:

$$
\left.\begin{aligned}
{}_{II}E_y &= \int A_{(k)} \cos\frac{\pi x}{a} e^{-iky} e^{-i\gamma_{(k)}z}\, dk \\
{}_{II}H_x &= \frac{-1}{\omega\mu_0}\int \gamma_{(k)} A_{(k)} \cos\frac{\pi x}{a} e^{-iky} e^{-i\gamma_{(k)}z}\, dk
\end{aligned}\right\}.
$$

where k is the transverse wave number with respect to y; γ_k - longitudinal wave numbers of each of the variants with respect to y.

We write the boundary conditions for E_y and H_x with z=0:

$$
\left.\begin{aligned}
E_0 \cos\frac{\pi x}{a} e^{im(y)\psi_0}(1+R_1) &= \int A_{(k)} \cos\frac{\pi x}{a} e^{-iky} dk \\
-\frac{\gamma}{\omega\mu_0} E_0 \cos\frac{\pi x}{a} e^{im(y)\psi_0}(1-R_1) &= -\frac{1}{\omega\mu_0}\int \gamma_{(k)} A_{(k)} \cos\frac{\pi x}{a} e^{-iky} dk
\end{aligned}\right\}. (1) \qquad (1)
$$

These boundary conditions are approximate, since the higher types of fields are not taken into account in region I.

We multiply the obtained equations by $e^{ik'y}$ and integrate for all y. Due to the orthogonality of the proper fields, only the components for which k=k' will remain on the right sides of equations (1). Then we obtain

$$
\left.\begin{aligned}
MbA_{(k')} &= E_0(1+R_1)\int e^{im(y)\psi_0} e^{ik'y} dy \\
Mb\gamma_{(k')}A_{(k')} &= E_0\gamma(1-R_1)\int e^{im(y)\psi_0} e^{ik'y} dy
\end{aligned}\right\}, \qquad (2)
$$

where M is the number of waveguides, Mb - total dimension of the antenna with respect to y. The integral on the right sides of (2) can be divided into the terms, which correspond to the individual waveguides. These terms will differ only in the phase factors, which depend on the waveguide number and on the angle of scan. Then the entire integral can be represented by the sum

$$
\int e^{im(y)\psi_0} e^{ik'y} dy = \sum_{m=0}^{M-1} e^{im(\psi_0+k'b)} \int_{-b/2}^{b/2} e^{ik'y} dy.
$$

After adding and integrating, we obtain the following system of equations:

$$
\left.\begin{aligned}
A_{(k')} &= E_0(1+R_1)\frac{\sin\frac{k'b}{2}}{\frac{k'b}{2}}\,\frac{\sin M\frac{\psi_0+k'b}{2}}{M\sin\frac{\psi_0+k'b}{2}} e^{i(M-1)\frac{\psi_0+k'b}{2}} \\
\gamma_{(k')}A_{(k')} &= \gamma E_0(1-R_1)\frac{\sin\frac{k'b}{2}}{\frac{k'b}{2}}\,\frac{\sin M\frac{\psi_0+k'b}{2}}{M\sin\frac{\psi_0+k'b}{2}} e^{i(M-1)\frac{\psi_0+k'b}{2}}
\end{aligned}\right\}. \qquad (3)
$$

We direct M towards infinity. In this case the factor $\frac{\sin M(\psi_0 - k'b)/2}{M \sin(\psi_0 + k'b)/2}$ tends towards unity with $k' = (2\pi p - \psi_0)/b$, where $p = -\infty \div \infty$, and becomes zero with all other values of k'. Thus, in an infinite system, k' has a discrete spectrum of values and not a continuous one.

From (3) we determine the amplitudes of the field components in region II

$$A_{(k')} = E_0 \frac{\sin \frac{k'b}{2}}{\frac{k'b}{2}} \frac{2\gamma}{\gamma + \gamma_{(k')}},$$

where

$$k' = \frac{2\pi p - \psi_0}{b}; \quad \gamma_{(k')} = \sqrt{\left(\frac{2\pi}{\lambda}\right)^2 - \left(\frac{\pi}{a}\right)^2 - (k')^2}.$$

It is possible to show that the waves with the following indices are the propagating ones:

$$p < \frac{\gamma b + \psi_0}{2\pi}; \text{ where } \gamma = \sqrt{\left(\frac{2\pi}{\lambda}\right)^2 - \left(\frac{\pi}{a}\right)^2}.$$

and only one wave with p=0 propagates when $\psi_0 < \pi$. The wave numbers for this field component:

$$k'_0 = -\frac{\psi_0}{b}; \quad \gamma_0 = \sqrt{\gamma^2 - \left(\frac{\psi_0}{b}\right)^2}. \tag{4}$$

Determining the reflection coefficient at the input of the system

Let us compose the scattering matrix of the transition from the system of waveguides to a system of parallel plates:

$$S = \begin{bmatrix} R_1 & T_{12} \\ T_{21} & R_2 \end{bmatrix}.$$

We will determine the elements of the scattering matrix of the transition approximately, taking into account only the propagating kinds of waves in the waveguides and in the system of parallel plates. In this case, boundary conditions (1) for the transverse components E_y and H_x of the field during the transition from region I to region II can be transformed to the form

$$\left.\begin{aligned}(1+R_1) &= T_{12},\\ \gamma(1-R_1) &= \gamma_0 T_{12}\end{aligned}\right\},$$

where T_{12} is the coefficient of transfer across the boundary. Similarly, for the reverse transition we obtain

$$\left.\begin{aligned}(1+R_2) &= T_{21}\\ \gamma_0(1-R_2) &= \gamma T_{21}\end{aligned}\right\}.$$

From this we determine the elements of the scattering matrix of the transition:

$$R_1=\frac{\gamma-\gamma_0}{\gamma+\gamma_0};\quad R_2=\frac{\gamma_0-\gamma}{\gamma+\gamma_0};\quad T_{12}=\frac{2\gamma}{\gamma+\gamma_0};\quad T_{21}=\frac{2\gamma_0}{\gamma+\gamma_0}.$$

The waves at the interface are shown schematically in Fig. 2.

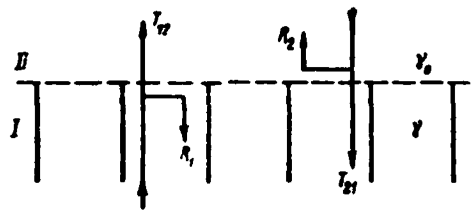

Fig. 2.

We will present this entire system in the form of a connection of five waveguide quadrupoles (Fig. 3). Here S_1 and S_5 are the matrices of transition from the system of waveguides to the system of parallel plates (I–II boundary):

$$S_1=S_5=\begin{bmatrix}R_1 & T_{12}\\ T_{21} & R_2\end{bmatrix}.$$

S_3 - scattering matrix of the reverse transition (II–III boundary):

$$S_3=\begin{bmatrix}R_2 & T_{21}\\ T_{12} & R_1\end{bmatrix}.$$

The second and fourth quadrupoles produce only a phase shift of the propagating wave; in this case, the transmission coefficient of the compensating section (region II) depends on the scan angle on the basis of (4). $S_2=\begin{bmatrix}0 & e^{i\gamma_0 l}\\ e^{i\gamma_0 l} & 0\end{bmatrix}$, while the scattering matrix S_4 of the waveguide array (region III) yields only the transfer of the plane of the terminals:

$$S_4=\begin{bmatrix}0 & e^{i\gamma l}\\ e^{-i\gamma l} & 0\end{bmatrix}.$$

Now we proceed to the transmission matrices of the quadrupoles, we determine a composite transmission matrix of the system $T=T_5T_4T_3T_2T_1$ and then a composite scattering matrix. In this case, for the reflection coefficient at the input of the system, we obtain

$$R=R_1+R_2T_{12}T_{21}e^{i2\gamma_0 l}+R_1T_{12}^2T_{21}^2e^{i(2\gamma_0 l+2\gamma d)}.$$

It is easy to show that when $\psi_0\leqslant\gamma_0\ T_{12}T_{21}\approx 1$. Then the reflection coefficient at the system's input

$$R=R_1[1-e^{i\alpha}+e^{i(\alpha+\beta)}],$$

where $\alpha=2\gamma_0 l$; $\beta=2\gamma d$.

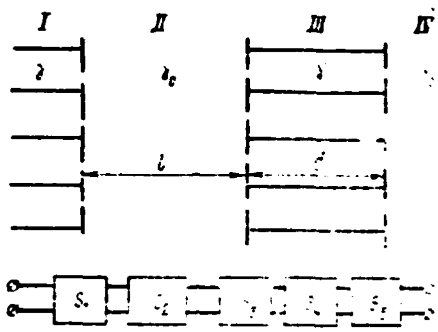

Fig. 3.

We define the square of the modulus of the reflection coefficient at the input as

$$|R|^2=|R_1|^2F(\alpha,\ \beta). \qquad (*)$$

Here

$$F(\alpha,\ \beta)=3-2\cos\alpha-2\cos\beta+2\cos(\alpha+\beta). \qquad (5)$$

Table 1

p		0	1	−1	2	−2	3	−3
$\frac{\lvert A_p\rvert}{E_0}$	$\psi_0=0$	1	0	0	0	0	0	0
	$\psi_0=\frac{\pi}{2}$	1,63	0,54	0,325	0,232	0,160	0,14[illegible]	0,124

Formula (5) is approximate, since only the propagating types of waves were taken into account in the waveguides and in systems of parallel plates. With an inphase excitation of the array, the plane wave passes through the entire system without distortions, and higher types of waves are not excited at the boundaries of the regions. When the phase shift between the adjoining radiators ψ_0 increases from 0 to γ_b, the amplitudes of the higher-type waves increase from zero to a certain value, which is shown in Table 1 for λ=3.2 cm, axb=2.3x1.0 cm^2.

Table 2

z, cm		0	0.1	0,3	0.5
$e^{-\Gamma_p z}$	$p=1$	1	0,64	0,26	0,10
	$p=-1$	1	0,46	0,10	0,02

Attenuation of waves with p=$\pm$1 along region II with $\psi_0=\frac{\pi}{2}$ is shown in Table 2.

Calculating the parameters of the matching scheme

The problem of coordination of the system is reduced to the minimization of the factor F(α, β). Calculation (see Fig. 4) shows that this function turns to zero, when $\alpha=\beta=\pi/3$.

The quantity $\alpha=2\gamma_0 l$ is a function of the phase shift in the array ψ_0; thus, assigning the value of ψ_0', at which $\alpha=\pi/3$, we thereby select the inclination angle of the beam at which $F(\psi_0')=0$. Since in the system without compensation the reflection coefficient R_1, beginning from zero with x=0, increases approximately as x^4, where $x=\psi_0/\gamma b$, the value of x' at which it is desirable to have F(x')=0 should be selected at the end of the working sector of angles $\psi_0=-\gamma b$–$+\gamma b$.

Fig. 5 shows the dependences |R(x)| for four versions: x'=0.6; 0.7; 0.8; and 0.9. It can be seen from the graphs that when x'=0.8, the coordination of the system improves significantly as compared with the original.

Example of Calculation

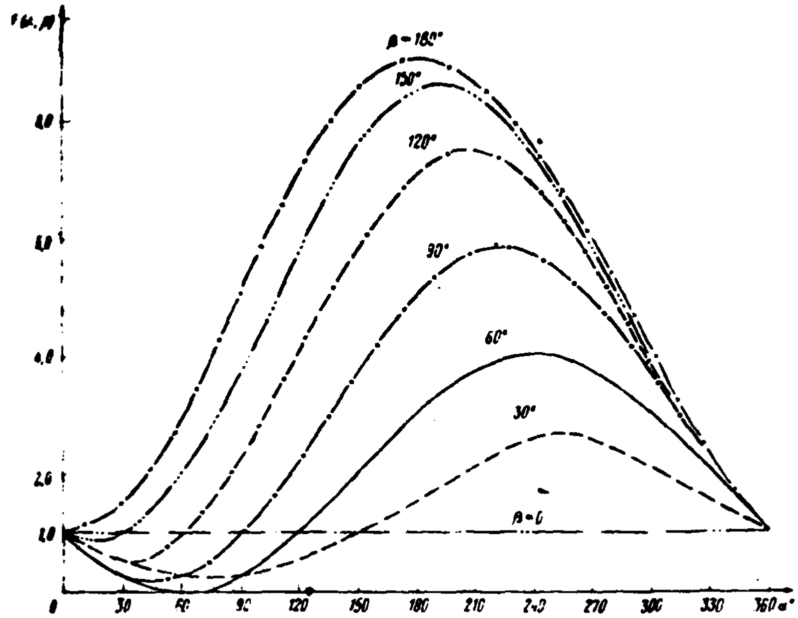
β = 180°
150°
120°
90°
60°
30°
β = 0
0
30
60
90
120
150
180
210
270
300
330

Fig. 4.

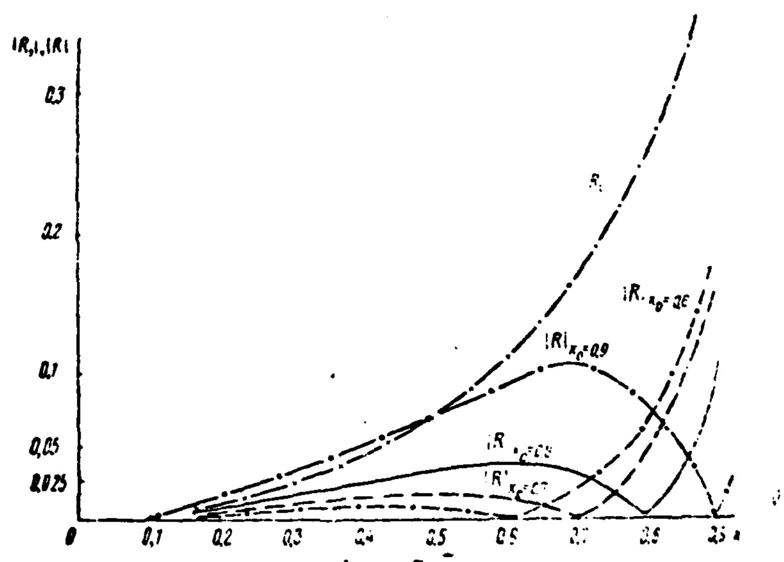
0,3
0,2
0,1
0,05
0,025
0
0,1
0,2
0,3
0,5

Fig. 5.

When $\lambda=3.2$ cm and $a\times b=2.3\times1.0$ cm^2, we obtain the distance from the aperture to the compensating region $d=\frac{\beta}{2\gamma}=3.7$ mm and the length of the compensating region $l=6.27$ mm.

In this case the reflection coefficient along the field is less than 5% in the interval $\psi_0=-71-71^\circ$. This corresponds to the scan sector $\Theta=-40-40^\circ$. In such a sector, for a system without compensation, the reflection coefficient reached 35% along the field (see Fig. 6).

In order to expand the scan sector, one can increase the width of waveguides. For example, with a=4.6 cm and $\Theta=-61-61^\circ$.

The parameters of the matching system, in this case, are: d=2.85 mm and $l=4.74$ mm.

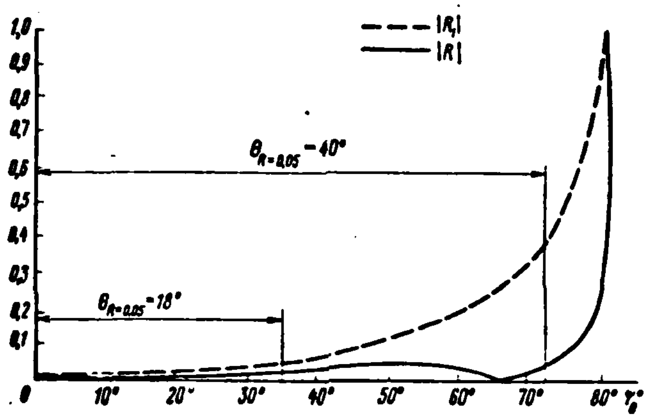

Fig. 6.

After differentiating all the frequency-dependent values in (*) with respect to λ, we obtain the following for the most dangerous case (edge of the interval $|x|=0.87\ \gamma b$):

$$\frac{\Delta|R|}{|R|} = -10{,}4\,\frac{\Delta\lambda}{\lambda}.$$

From this we find that by increasing the frequency by 2%, the maximum reflection coefficient along the field becomes equal to 6% instead of 5% when f=9370 MHz.

Conclusion

The calculation has shown that the system examined for the excitation of an array decreases, to a considerable extent, the change in

the reflection coefficient at the system's input when scanning over a wide sector. The coordination of the array improves significantly. With a phase shift between the adjoining elements $\psi_0=-0.87\ \gamma b-0.87\ \gamma b$, the maximum reflection coefficient along the field decreases, as compared with the system without compensation, from 35% to 5%; in this case, the value of the kbv [traveling-wave ratio] increases from 0.48 to 0.91.

Received
11/06/69.

Bibliography

1. Hannan P. W., Lerner D. S., Knittel G. H. Impedance Matching a Phased—Array Antenna over Wide Scan Angles by Connecting Circuits. IEEE Transactions on Antennas and Propagation, 1965, AP—13, № 1.

2. O. G. Vendik, L. V. Ryzhkova. Synthesis of a circuit for compensating the interconnection of radiators in a phased antenna array. Antennas under the editorship of A. A. Pistol'kors. Issue 4. M., "Svyaz'" [communication], 1968.

3. L. V. Ryzhkova. Compensation of the direct and feedback interconnection in an indefinite line. Antenna under the editorship of A. A. Pistol'kors. Issue 8, M., "Svyaz'", 1970.

4. L. V. Ryzhkova. Simultaneous compensation of the direct and feedback interconnection of radiators in an idefinite array. Antennas under the editorship of A. A. Pistol'kors. Issue 8, M., "Svyaz'", 1970.

Received

11/VI/69.

CALCULATION OF THE RADIATION CHARACTERISTICS OF HIGHLY DIRECTIONAL ARC ANTENNAS

A. A. Kuz'min

This article examines the radiation patterns of high-directional arc-antenna array (DAR). Simple relations were obtained for calculating the width of the main beam, position, and size of the aperture side lobes of DAR with isotropic radiators, which are excited uniformly.

Introduction

Much attention has been devoted in recent years to the axisymmetrical antenna arrays (circular, spherical, conical) [1, 2, 3, 4, 5 and other], which is explained by a number of advantages of such antennas [2] over the plane antenna arrays. Arc antenna array (DAR) are the integral part of the axisymmetric antennas. Calculation of the high-directional ($R \gg \lambda$) DAR is reduced primarily to determining the form of the radiation pattern and the directivity factor (knd) depending on the nature of the amplitude distribution of currents through the radiators at a given phase distribution. There are no fundamental difficulties in calculating the radiation properties of DAR using the known amplitude-phase current distributions. This calculation can be performed using the expressions for the radiation patterns of the high-directivity DAR, obtained using the methods of an equivalent aperture and a stationary phase [1], or by the expressions, which are similar for the linear antennas.

However, these expressions are quite cumbersome to use for an

analysis and they require the use of a digital computer for calulation.

Today simple expressions are available which are convenient to use in the engineering practice for calculating the radiation characteristics of DAR with the angular apertures $0^\circ<2\beta<180^\circ$; these expressions were derived on the basis of the synthesis method, which uses the conversion of a nonuniform antenna array to an equivalent radiator with a continuous distribution of amplitudes, which has been worked out most comprehensively in the works of A. Ishimaru [6, 7].

General Relations

For the convenience of further formulation, we will consider an arc AR [antenna array] arranged in a rectangular system of coordinates in such a way that its diametric plane is horizontal. Let us assume that the antenna (Fig. 1) consists of N radiators, which are arranged uniformly along the arc with the angular aperture 2β and radius R. Then the angular distance between the radiators equals 0, $\frac{2\beta}{N}$, $\frac{4\beta}{N},\ldots,\frac{2(N-1)\beta}{N}$.

It is not difficult to obtain an expression from Fig. 1 for determining the phase change between the DAR's radiators, which is caused by the difference in the travel of the beams to the point in space. Taking into account the electrical phase compensation to ensure inpahse addition of the fields of all the radiators in the direction φ_0, Θ_0 has the form

$$\psi_l(\varphi, \Theta) = KR[(1-\cos l\alpha)\times(v-v_0)+\sin l\alpha\,(u-u_0)] \tag{1}$$

where

$$u=\sin\varphi\cos\Theta,$$
$$u_0=\sin\varphi_0\cos\Theta_0,$$
$$v=\cos\varphi\cos\Theta,$$
$$v_0=\cos\varphi_0\cos\Theta_0.$$

We present expression (1) in the form

$$\psi_l(\varphi, \Theta)=\xi_l(\varphi, \Theta)+\Delta\xi_l(\varphi, \Theta). \tag{2}$$

The first term on the right side of equality (2)

$$\xi_l(\varphi, \Theta)=KR\sin l\alpha\,(u-u_0) \tag{3}$$

represents a phase factor for the radiation pattern of a nonuniform

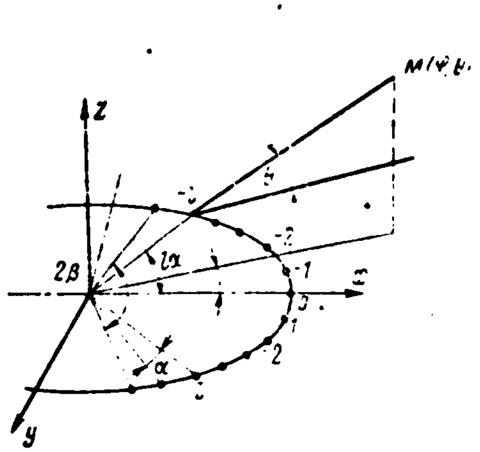

Fig. 1.

antenna with the rule governing the arrangement of the radiators in the form

$$d_l = R\sin l\alpha. \qquad (4)$$

We will call function (3) the phase factor of the radiation pattern of a nonuniform antenna radiating transversely. However, the second term

$$\Delta\xi_l(\varphi,\,\Theta) = KR(1-\cos l\alpha)(v-v_0) \qquad (5)$$

characterizes the phase change caused by the difference in the traveling of beams from the radiators of the DAR and the corresponding elements of a nonuniform antenna, which is equivalent to it and radiating transversely. Accordingly, we call function (5) the phase factor of the radiation pattern of a nonuniform antenna radiating longitudinally with the rule governing the arrangement of radiators in the form

$$d_l' = R(1-\cos l\alpha). \qquad (6)$$

It follows from work [1] and relations (1), (3), and (5) that the radiation pattern of DAR can be viewed as the radiation pattern of an equivalent nonuniform AR with the phase distribution, which is different from the inphase distribution by the value $\Delta\xi(\varphi,\theta)$.

In view of this fact, we use the conversion of the nonuniform array to an equivalent radiator with a continuous distribution of amplitudes to calculate the radiation characteristics of the DAR [6, 7].

We will obtain a number of auxiliary relations coupled with the presentation of formulas (4) and (6) in the form [6]:

$$w = s + g(s), \tag{7a}$$
$$t = B_1 s + \eta(s), \tag{7b}$$

where w and t are normalized functions of the position of the radiators of the nonuniform antennas radiating transversely and longitudinally, respectively; B_1 - constant coefficient; s - normalized "function of the radiator number"; $g(s)$ and $\eta(s)$ characterize the deviations in the arrangement of radiators in nonuniform AR from a uniform arrangement. Normalization is performed such that $w=\pm 1$, $t=B_1$, with s=$\pm$1, while the corresponding deviations $g(\pm 1) = \eta(\pm 1) = 0$.

If we present the right parts of functions (4) and (6) in the form of a sum of two terms, one of which characterizes the arrangement of the radiators in an equally spaced linear AR and the other - deviation of the radiator arrangement in an unequally spaced AR from a uniform arrangement, and assume that N→∞, then formulas (4) and (6) will be written in the form

$$w(s) = s + (\sin\beta s/\sin\beta - s) = s + g(s), \tag{8}$$
$$t(s) = B_1 s + [(1-\cos\beta s) - B_1 s] = [B_1 s + \eta(s)], \tag{9}$$

respectively, where B_1 is a constant coefficient, which depends only on the value of 2β.

The values of the coefficient B_1, as it ensues from formula (6), can be determined from the relation

$$B_1 = 1 - \cos\beta. \tag{10}$$

For the convenience of further presentation, we present the rules and of the deviation of the arrangement of the radiators from a uniform arrangement in the form:

$$g(s) = \sin\beta s/\sin\beta - s = B\sin\pi s, \tag{11}$$
$$\eta(s) = (1-\cos\beta s) - (1-\cos\beta)s = -B_2\sin\pi s, \tag{12}$$

respectively.

Using the approximation via the method of least squares, it is easy find that equalities (11) and (12) will be valid if

$$B = \frac{2}{\pi}\frac{(\beta/\pi)^2}{1-(\beta/\pi)^2}; \quad B_2 = (1+\cos\beta)\frac{2}{\pi}\frac{(\beta/\pi)^2}{1-(\beta/\pi)^2}. \tag{13}$$

In this case the value of the mean square error is less than 5%.

As a result of these transformations, the phase factor (1) of the radiation pattern of the DAR, which was converted to an equivalent radiator with a continuous distribution, will assume the form

$$\psi(\varphi, \Theta, s) = (s + B\sin\pi s)(U - U_0) + (B_1 s - B_2\sin\pi s)(V - V_0). \tag{14}$$

Here:

$$\begin{gathered} U = KR\sin\beta\sin\varphi\cos\Theta;\quad U_0 = KR\sin\beta\sin\varphi_0\cos\Theta_0; \\ V_0 = KR\cos\varphi_0\cos\Theta_0;\quad V = KR\cos\varphi\cos\Theta. \end{gathered} \tag{15}$$

<u>Derivation of an expression for the radiation pattern of a DAR</u>

The known expression for the radiation pattern of a DAR consisting of N radiators whose directivity is described by the function $F_1(\varphi, \theta, \alpha)$ and amplitude distribution $\{I_l\}$. has the following form:

$$G(\varphi, \Theta) = \sum_{l=-n}^{n} I_l F_1(\varphi, \Theta, \alpha) e^{i\psi_l(\varphi, \Theta)}, \tag{16}$$

where $\psi_l(\varphi, \theta)$ is the phase factor defined by formula (1).

As was shown in work [6], summation of series (16) can be accomplished by using the Poisson's summation formula. In this case, series (16), with the selection of the origin of the coordinates at the center of AR and the total length of the aperture normalized to 2, is presented as

$$G(\varphi, \Theta) = \sum_{m=-\infty}^{\infty} (-1)^{m(N-1)} G_m(\varphi, \Theta), \tag{17a}$$

$$G_m(\varphi, \Theta) = \frac{1}{2}\int_{-1}^{1} I(s) F_1(\varphi, \Theta, s) e^{-it(s)(V-V_0) + i\omega(s)(U-U_0) + imN\pi s} ds, \tag{17b}$$

where $\omega(s)$ and $t(s)$ are the normalized functions of the position of the radiators, defined by formulas (8) and (9), respectively. Substituting formulas (8), (9), (11), and (12) in (17b) and assuming that $F_1(\varphi, 0, s) = 1.0$; I(s)=1.0, we obtain

$$G_m(\varphi, \Theta) = \frac{1}{2}\int_{-1}^{1} e^{-i(V-V_0)(B_1 s - B_2\sin\pi s) + i(U-U_0)(s + B\sin\pi s) + imN\pi s} ds. \tag{18}$$

Taking into account the even symmetry of the function t(s) and after a series of transformations, integral (18) is written as follows by means of the Anger and Lommel-Weber functions:

$$G_m(\varphi, \Theta) = \frac{1}{2}\{A_{\nu-mN}(z) + A_{\nu_1+mN}(z_1) + i[E_{\nu-mN}(z) + E_{\nu_1+mN}(z_1)]\}, \tag{19a}$$

where $A_\nu(z)$, $E_\nu(z)$ are the Anger and Lommel-Weber functions, respectively, defined in work [10]:

$$\left.\begin{array}{ll} \nu_1=\dfrac{B_1(V-V_0)+(U-U_0)}{\pi}, & \nu=\dfrac{B_1(V-V_0)-(U-U_0)}{\pi} \\ z_1=B_2(V-V_0)-B(U-U_0), & z=B_2(V-V_0)+B(U-U_0) \end{array}\right\}. \tag{19b}$$

Substituting formula (19a) in series (17a), we obtain an expression for a three-dimensional radiation pattern of a DAR, presented in terms of the Anger and Lommel-Weber functions:

$$G(\varphi, \Theta)=G_0(\varphi, \Theta)+\sum_{m=1}^{\infty}(-1)^{m(N-1)}[G_m(\varphi, \Theta)+G_{-m}(\varphi, \Theta)], \tag{20}$$

where

$$G_0(\varphi, \Theta)=\frac{1}{2}\{A_\nu(z)+A_{\nu_1}(z_1)+i[E_\nu(z)+E_{\nu_1}(z_1)]\}. \tag{21}$$

As it follows from formulas (20 and 21), the radiation pattern of the DAR is presented in the form of two addends, of which the first describes the directed properties of the DAR with a continuous aperture and the second determines the deviation of the radiation pattern, caused by the discreteness of arrangement of the radiators. Let us examine the characteristics of the DAR's directivity in two mutually perpendicular planes: in the plane of the arc (plane xoy) and in the plane of a normal plane (plane xoz).

Analysis of radiation pattern of a DAR with a continuous aperture in the arc plane

As it follows from the preceding section, the formula $G_0(\varphi, \theta)$ for the radiation pattern of the DAR with a continuous aperture ($N\to\infty$) is obtained from formula (19a) by substitution m=0 and has the form

$$G_0(\varphi, 0)=\frac{1}{2}\{A_\nu(z)+A_{\nu_1}(z_1)+i[E_\nu(z)+E_{\nu_1}(z_1)]\}. \tag{22}$$

Since the Anger and Lommel-Weber functions are tabulated in [9], it is much easier to calculate the radiation pattern by formula (22) than by the expression obtained by means of an equivalent aperture [1].

Furthermore, taking into account that [10]

$$A_{-\nu}(z)=A_\nu(-z), \quad E_{-\nu}(z)=-E_\nu(-z),$$

the following equation is valid for calculating the main beam and the aperture side lobes of highly directional DAR:

$$G'_0(\varphi) = A_{\frac{U}{\pi}}(-BU). \qquad (23)$$

Radiation patterns (main beam and aperture side lobes) calculated by formula (23) for the various values of $\frac{\nu}{z} = -\frac{1}{\pi B} = b$, are shown in Fig. 2.

The analysis of (23) and the curves presented in Fig. 2 shows that the form of the DAR's radiation pattern depends substantially on the selection of the parameters R and β.

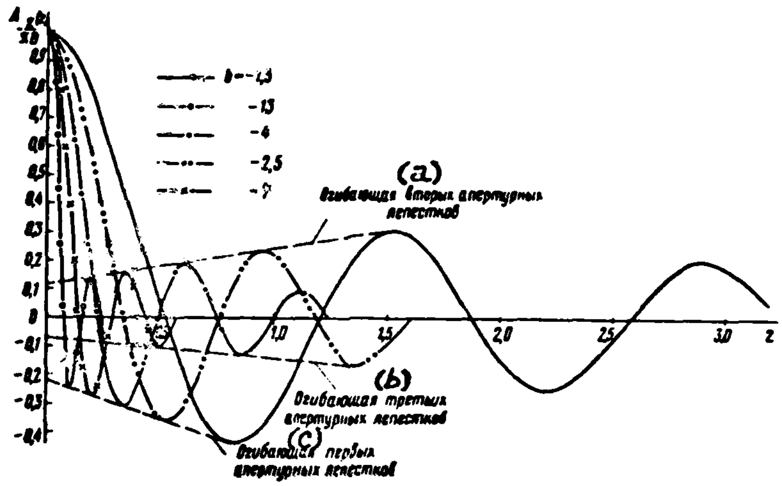

Fig. 2.

KEY: (a) Envelope of the second aperture lobes. (b) Envelope of the third aperture lobes. (c) Envelope of the first aperture lobes.

Since the inequality $|z|<|\nu|$ is fulfilled for the φ values, which are within the width of the radiation pattern $2\Delta\varphi_0$, with respect to the first zeros and, furthermore, the z and ν are small with respect to the absolute value, then using an asymptotic expansion of the Anger function [10] and having retained only the first terms of the series we obtain

$$G'_0(U) = \frac{\sin U}{U}\,\frac{1 - U^2/\pi^2(1 + \pi B)}{1 - U^2/\pi^2}. \qquad (24)$$

The first cofactor of the obtained expression describes the radiation pattern of a uniform linear AR, while the second takes into account the specific properties (curvature) of the DAR.

In this case, it is easy to see that the second factor for the region of the angles of the main beam ($U<\pi$) will be less than unity.

This attests to the fact that the main beam of the DAR is narrower than the main beam of a linear antenna with the same aperture. The patterns of both antennas coincide with a decrease in the angular aperture 2β of the DAR.

The width of the main beam of the DAR is defines from expression (24) as:

a) using nulls

$$2\Delta\varphi_0^0 = \frac{57{,}3\lambda}{R\sin\beta\sqrt{1+\pi B}}. \quad (25a)$$

b) using level 0.5 G^2_{max}

$$2\Delta\varphi^{\circ}_{0,5} = \frac{27\lambda}{R\sin\beta\sqrt{1+\pi B}}. \quad (25b)$$

Expression (23) also makes it possible to explain the behavior of the (aperture) side lobes.

For this, on the basis of the solution of $A_{-\frac{z_{0p}}{\pi B}}(z_{0p})=0$ and Fig. 2, graphs were constructed for the position z_{0p} of the zeros of the function $A_{-\frac{u}{\pi}}(BU)$ in the range $0<z\leqslant 3$ depending on the number of p (Fig. 3). As can be seen from Fig. 3, dependences $z_{0p}=f(p)$ have the form of straight lines for the various values of 2β; in this case, all lines intersect at the same point D with the coordinates $(\frac{1}{4}, 0)$. Analytically, dependences $z_{0p}=f(p)$ are exprassed by the relation

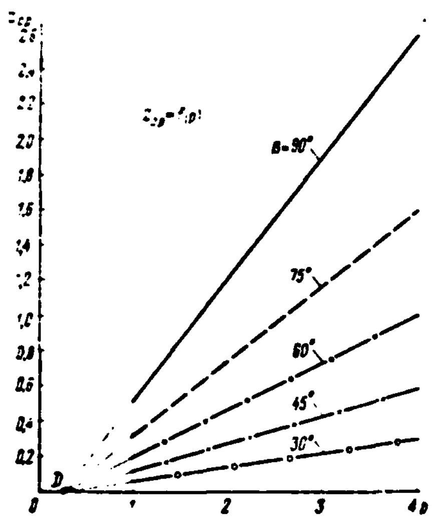

Fig. 3.

$$z_{0p} = 1{,}04B\frac{\pi}{4}(4p-1), \quad (26)$$

where $B=\frac{2}{\pi}\,\frac{(\beta/\pi)^2}{1-(\beta/\pi)^2}$.

Having p rmitted the maxima of the function $A_{-\frac{u}{\pi}}(BU)$ in the first approximation to arrange symmetrically between the corresponding zeros, from formula (26) the position of the maxima of the aperture side lobes of the DAR's radiation pattern are defined as

$$\varphi_{max} = \arcsin\left(1{,}04\lambda\frac{4p+1}{8R\sin\beta}\right). \quad (27)$$

The calculations have shown that for determining the position of the maxima of the aperture side lobes, the error of formula (27) does not exceed 2.5%.

Having substituted formula (27) in formula (23), it is possible to find the values of the aperture side lobes of the DAR with the various values of 2β:

$$G_{\text{макс}}(\beta)=A_{\frac{4p+1}{3,85}}\left(-\pi B\frac{4p+1}{3,85}\right). \tag{28}$$

It follows from expression (28) that the value of the aperture side lobes is determined only by the angular aperture 2β of the antenna. It is interesting to note that the maxima of the aperture side lobes approach the values of the corresponding lobes of a uniform linear antenna with a decrease in the value of 2β. The latter is explained by a decrease in the density concentration of the radiated energy at the edges of the antenna.

<u>Effect of a finite number of radiators on the DAR's radiation pattern in the arc plane</u>

Distrortions of the radiation pattern caused by a finite number of radiators are described by the series

$$\begin{aligned}G_{\text{укл}}(\varphi)=\frac{1}{2}\sum_{m=1}^{\infty}(-1)^{m(N-1)}\{A_{\nu-mN}(z)+A_{\nu+mN}(z)+A_{\nu_1-mN}(z_1)+\\+A_{\nu_1+mN}(z_1)+i\,[E_{\nu-mN}(z)+E_{\nu+mN}(z)+E_{\nu_1-mN}(z_1)+E_{\nu_1+mN}(z_1)]\}.\end{aligned} \tag{29}$$

As is known [6], when the below inequalities are satisfied

$$\left.\begin{aligned}|\nu-mN|>|z|,\quad |\nu+mN|>|z|\\ |\nu_1-mN|>|z_1|,\quad |\nu_1+mN|>|z_1|\end{aligned}\right\} \tag{30}$$

the values of the Anger and Lommel-Weber functions are negligibly small, then, as one can see, the approximation $\varphi\approx(4\div5)\Delta\varphi_0$ is valid in the region of angles $G_{\text{укл}}(\varphi)\approx 0$. Thus, to calculate the main beam and the aperture side lobes of the DAR with a finite number of radiators, we can use the formulas and graphs obtained in the preceding section. Let us now examine the conditions for the fulfillment of inequalities (30) in the region of angles which are removed considerably from the main beam $(\varphi>5\Delta\varphi_0)$.

After substituting the values of ν, ν_1, z, z_1 in (30), it is easy to

see that the first and fourth inequalities are satisfied for the entire range of change in U and V, while the second and third, respectively, assume the form

$$\begin{aligned}&|B_1(V-V_0)-(U-U_0)+mN\pi| > \pi|B_2(V-V_0)+B(U-U_0)||\\&|B_1(V-V_0)+(U-U_0)-mN\pi| > \pi|B_2(V-V_0)-B(U-U_0)||\end{aligned} \qquad (31)$$

In order for the parasitic diffraction lobes to be absent, inequalities (30) must be fulfilled over the entire range of change in the values of U, U_0, V, and V_0, i.e.:

$$\begin{aligned}&-KR\sin\beta \leqslant U \leqslant KR\sin\beta, \quad -KR \leqslant V \leqslant KR,\\&-KR\sin\beta \leqslant U_0 \leqslant KR\sin\beta, \quad -KR \leqslant V_0 \leqslant KR.\end{aligned}$$

We note that the first part of inequalities (31) assumes the maximum value with the values:

$$V=V_0=0, \quad U=-U_0=KR\sin\beta. \qquad (32a)$$

Taking into account conditions (32a), it is easy to show that inequalities (31) are satisfied if

$$d<\frac{\lambda}{2}\,\frac{\beta}{\sin\beta\,(1+\pi B)}. \qquad (32b)$$

In this case, the second factor in the right side of (32b) for $0\leqslant\beta\leqslant1.57$

$$\frac{\beta}{\sin\beta\,(1+\pi B)}\approx 1{,}0.$$

Consequently, the condition for the absence of the parasitic diffraction lobes in the DAR with a finite number of radiators is the fulfillment of the inequality $d<\frac{\lambda}{2}$, which coincides with an analogous condition for the linear and circular [3] AR. It is obvious that with $d<\frac{\lambda}{2}$ the radiation patterns of the DAR can be calculated by formula (22).

If $d>\frac{\lambda}{2}$, parasitic lobes appear in the radiation pattern which are calculated by the formula

$$G_{yxn}(\varphi)=\frac{1}{2}\sum_{m=1}^{\infty}(-1)^{m(N-1)}\{A_{\nu+mN}(z)+A_{\nu_1-mN}(z_1)+ i\,[E_{\nu+mN}(z)+E_{\nu_1-mN}(z_1)]\}. \qquad (33)$$

Formula (33) differs from (29) by the absence of the terms of the Anger and Lommel-Weber function with the orders $\nu-mN$ and ν_1+mN; since their values are negligibly small. Series (33) is a rapidly converg-

ing one.

This is easy to show if we consider the inequalities

$$|\nu+mN|<|z|,\quad |\nu_1-mN|<|z_1|, \tag{34a}$$

with the fulfillment of which the value of deviation $G_{\text{укл}}(\varphi)$ will be considerable.

Having performed the transformations with inequalities (34a) which are analogous to the preceding case, it is possible to obtain the conditions for their fulfillment accordingly:

$$d\geqslant\frac{m\lambda\beta}{(B_1+\pi B_2)(1-\cos\varphi)+\sin\beta(1-\pi B)\sin\varphi},\qquad d\geqslant\frac{m\lambda\beta}{\sin\beta(1+\pi B)\sin\varphi-(B_1-\pi B_2)(1-\cos\varphi)}. \tag{34b}$$

Since the right sides of inequalities (34b) assume the minimal value when $\varphi_{-1}=90^\circ$ they can be rewritten in the form:

$$d>\frac{m\lambda\beta}{(B_1+\pi B_2)+\sin\beta(1-\pi B)},\quad d\geqslant\frac{m\lambda\beta}{\sin\beta(1+\pi B)-(B_1-\pi B_2)}. \tag{34c}$$

When $\beta\to 0$, a know relation $d=\lambda$ ensues from (34c) - which is the condition for the appearance of the diffraction lobe in the direction $d\approx\lambda$, in a linear AR. The analysis of (34c) also shows that it is sufficient to limit oneself to one-two (m=1.2) terms in sum (33) to calculate the distortion of the DAR's radiation pattern caused by the discreteness of arrangement of the radiators with $d\approx\lambda$, i.e.,

$$G_{\text{укл}}(\varphi)=\frac{1}{2}\sum_{m=1}^{2}(-1)^{m(N-1)}\{A_{\nu+mN}(z)+A_{\nu_1-mN}(z_1)+ + i[E_{\nu+mN}(z)+E_{\nu_1-mN}(z_1)]\}. \tag{35}$$

To illustrate this analysis, an example is given in Fig. 4a, b for calculating the radiation pattern and its components for the DAR with the following parameters: KR=30, N=11, $d=\lambda$, $2\beta=125.4^{\circ}$, and $F_1(\varphi)=1.0$. For a comparison, the radiation pattern was calculated on both the digital computer "Ural-2" (Fig. 4b, solid line) using formula (16) and by the expressions (22) and (35) obtained anew (the calculation points in Fig. 4b are indicated by crosses).

In this case, in order to show the effect of radiation $G_0(\varphi)$ of a continuous arc antenna and the distortion caused by the presence of

a finite number of radiators on the formation of the radiation pattern, their calculation was performed individually (Fig. 4a). Fig. 4b also

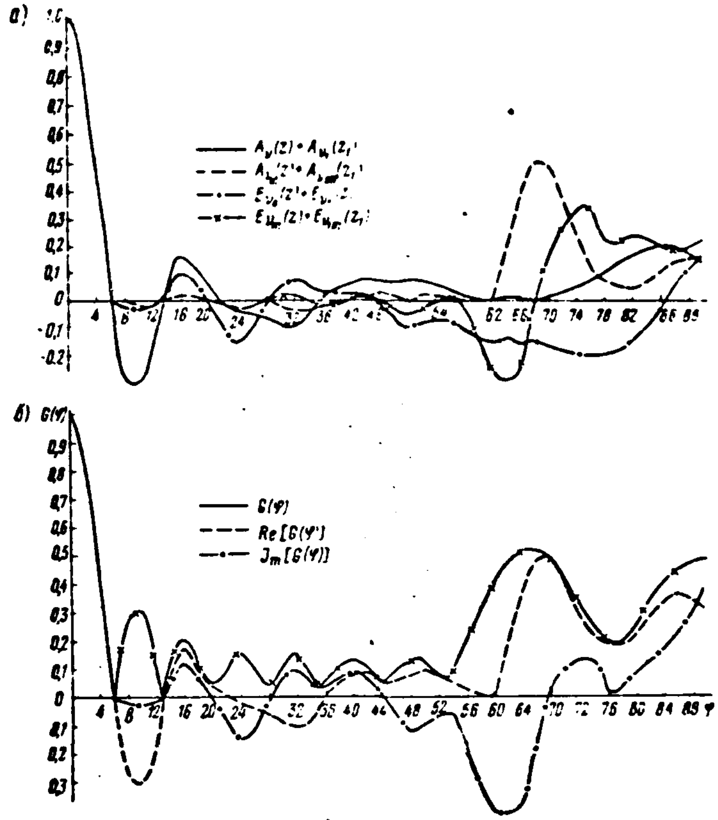

Fig. 4.

shows the combined real and imaginary components of DAR's radiation pattern. These curves show clearly two regions of the radiation pattern: region of the main beam and aperture side lobes ($\varphi<16°$) and region of the diffraction lobe ($54°\leq\varphi\leq76$).

The analysis of the curves shows that the main beam and the aperture side lobes of an arc AR are determined, primarily, by the real radiation-pattern component of a continuous arc antenna, while the distortions introduced by the discreteness of arrangement of the radiators are virtually zero. With a further increase in the angles $\varphi>16°$, the discreteness of arrangement of the radiators begins to affect the form of the radiation pattern of the DAR which, in the region of angles $54°\leq\varphi\leq76°$, which causes a rather significant in size (≈50% along the field) diffraction lobe with a maximum at $\varphi\approx65°$. It should be noted

that the calculation of the distortions, which are caused by a finite number of radiators arranged at the interval $d \approx \lambda$, was performed using formula (35). In this case, as can be seen from Fig. 4b, the agreement between the results obtained from the calculations performed on a digital computer and manually is good.

Thus, the calculation that was performed confirmed the validity of the assumptions made earlier in the derivation of relations (23), (25), (34) and other for calculating the radiation characteristics of DAR.

Analysis of the radiation pattern of a DAR in the vertical plane

For most of the cases realized in practice, it is necessary to ensure the displacement of the main beam of a DAR only in the arc plane; therefore, it is advisable to assume that $\theta_0=0$. Furthermore, to simplify the analysis of the vertical radiation pattern, we will assume that the maximum of the main beam in the arc plane has the direction $\varphi_0=0$. Under these conditions, the vertical radiation pattern, as it follows from formula (20), is written as

$$G(\Theta)=A_{\nu_0}(z_0)+\mathrm{i}E_{\nu_0}(z_0)\sum_{m=1}^{\infty}(-1)^{m(N-1)}\{A_{\nu_0-mN}(z_0)+A_{\nu_0+mN}(z_0)+ \\ +\mathrm{i}[E_{\nu_0-mN}(z_0)+E_{\nu_0+mN}(z_0)]\},$$

where

$$\left.\begin{aligned}\nu_0=\frac{B_1}{\pi}(V-V_0);\quad V_0=KR\cos\Theta\\ z_0=B_2(V-V_0);\qquad V_0=KR\end{aligned}\right\}. \tag{36}$$

If the DAR with a relatively large number of radiators ($N\to\infty$) are used, which is such that $N>\nu_{0\max}$, the vertical radiation pattern of such an array is written as

$$G_0(\Theta)=A_{\nu_0}(z_0)+\mathrm{i}E_{\nu_0}(z_0). \tag{37}$$

It follows from formula (37) that when $\beta\to 0$, the radiation pattern $G_0(\theta)$ approaches that of the isotropic pattern [$A_0(0)=1$, $E_0(0)=0$], which corresponds to the case of a linear antenna. Furthermore, since for the relatively small angles θ ($\theta\approx\pm 20^0$) $\cos\theta\approx 1$, it can easily be seen from expression (37) that the form of the vertical radiation pattern corresponding to the arc factor is close to that of a plateau. The last position coincides with the results of work [8].

If we take into account that the ratio $\frac{\nu_0}{z_0}$ remains constant in

magnitude when β=const and $A^{*}_{\nu_0}(z_0)+E^{*}_{\nu_0}(z_0)=0.5$ when $z_0=\frac{\beta_1}{\pi}KR(1-\cos\theta)\approx 0.85$, then the width of the radiation pattern corresponding to the factor of the arc, at a level of half the power, is defined as

$$2\Delta\Theta_{0.5}=2\arccos\left[1-\frac{0.85\pi}{KR(1-\cos\beta)}\right]. \qquad (38)$$

The calculations have shown that the accuracy of formula (38) is higher than that of the corresponding relation obtained in work [8] and comprises a value of ≈2%.

Having performed the calculations, which are analogous to the preceding section, it is possible to show that the number of terms m that should be taken into account in the second term on the right side of formula (36) that characterizes the effect of the discreteness of arrangement of the radiators on the form of the vertical radiation pattern, is determined by the inequality

$$m\leqslant\frac{d}{\lambda}\,\frac{1-\cos\beta+\frac{\beta^{3/2}}{3}}{\beta}. \qquad (39)$$

It follows from inequality (39) that its fulfillment for m=const depends on the ratio d/λ and the quantity 2β of the DAR. Thus, for example, for the cases m=1 and m=2 the fulfillment of inequality (39) is determined by the dependences d/λ=f(β) (Fig. 5). In Fig. 5 the region located below the curve corresponding to m=1 shows that in the first approximation the radiation pattern G(θ) of a DAR with d/λ<1 corresponds to the radiation pattern of the DAR with a continuous aperture and, consequently, formula (37) is valid for this domain of values for d/λ. For the ratio d/λ lying within 1≤d/λ≤1.5, as it follows from the shaded area (Fig. 5), it is enough to limit oneself to one-two terms in sum (36), i.e.,

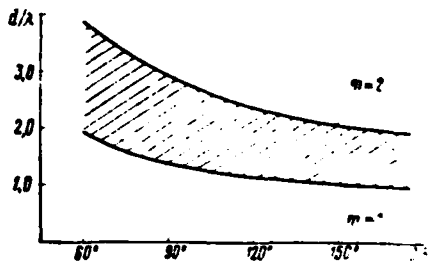

Fig. 5.

$$G_{\text{укл}}(\Theta)=\sum_{m=1}^{2}(-1)^{m(N-1)}[A_{\nu_0-mN}(z_0)+iE_{\nu_0-mN}(z_0)]. \qquad (40)$$

A series of calculations were performed to verify the correctness of the assumptions used in analyzing the radiation patterns.

Figures 6 and 7 show the vertical radiation patterns of a DAR with the angular aperture 2β=90 and 180 , respectively, calculated on a digital computer using formula (16) (for the case φ=0). In this case,

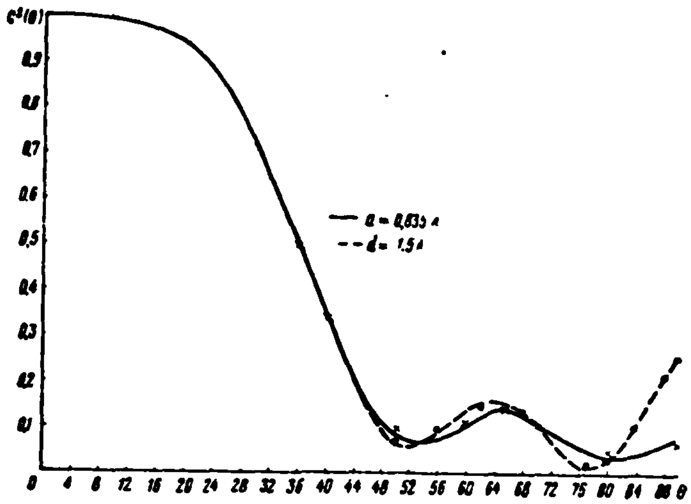

Fig. 6.

the period at which the radiators were arranged comprised d=0.835λ and 1.5λ for each value of 2β. The points calculated by fornula (37) are indicated by crosses on the patterns shown.

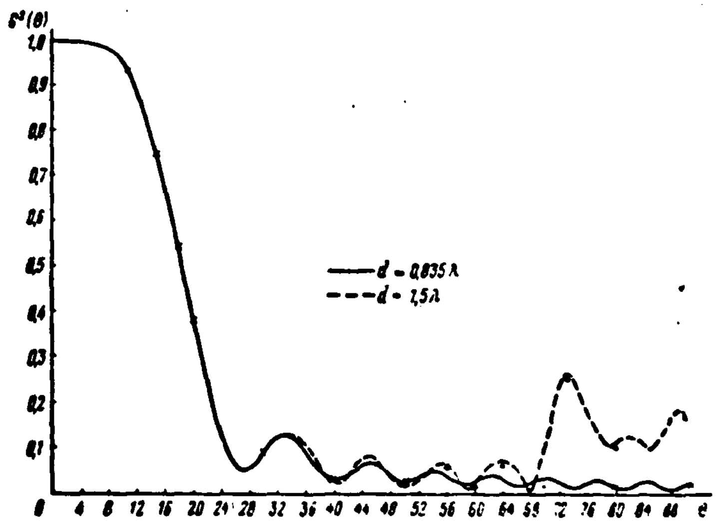

Fig. 7.

It can be seen from the comparison of the calculated values that the final number of radiators virtually has no effect on the form of the vertical pattern corresponding to the arc factor for the distances $d=0.835\lambda$. Good coincidence is observed with an increase in the distance between the radiators for the radiation patterns corresponding to $d=0.835\lambda$ and 1.5λ within the angles $0\leqslant\theta\leqslant50^0$. In the region of angles $\theta>50^0$, the radiation pattern is calculated by formulas (37) and (40) (in Figs. 6 and 7, these values are indicated by dots). As can be seen from Figs. 6 and 7, taking into account just terms in sum (36) ensures good agreement between the results derived from the calculation of the radiation patterns by the original and approximate formulas.

Thus, the conclusions obtained on the basis of the analysis of expression (36) are in good agreement with the results of the calculations performed.

Conclusions.

1. The approach examined for calculating the radiation characteristics of DAR, which is based on the presentation of the radiation pattern in series of the Anger and Lommel-Weber functions, makes it possible to obtain very simple relations for determining the width of the main beam, magnitude of the aperture side lobes, and their angular position depending on the geometrical dimensions of the arc R, 2β and thus simplify the engineering calculation of such antennas considerably.

It was shown that the magnitude of the aperture side lobes depends only on the values of 2β of a DAR.

2. This method can also be applied for calculating other AR that are not plane, arranged on bodies of revolution.

Bibliography

1. D. I. Voskresenskiy, A. I. Gudzenko. "Radiation Patterns of Arc Antennas." VUZ bulletins, USSR - radio engineering, vol. VIII, 1965, # 5, 574-580.

2. D. I. Voskresenskiy. Switching antennas with a wide-angle electric scan. VUZ bulletin, USSR - radio engineering, vol. 6, 1963, # 6.

3. Iames P. W. Polar patterns of phase-corrected circular arrays. Electronics Record, oct. # T-5, 1965.

4. D. I. Voskresenskiy, A. I. Gudzenko. Range nature of highly directional arc antenna arrays. VUZ bulletin, USSR - radio engineering, ser. X, 1967, # 2, 127-133.

5. D. I. Voskresenskiy, A. I. Gudzenko. Switching arc and spherical antenna arrays. VUZ bulletins, USSR - radio engineering, vol. XI, 1968, # 5, 44-451.

6. Ishimaru. Thinning and Broading Antenna Arrays by Unequal Spacings. IEEE. Trans on Antenna and Propag., v. AP—13, № 1, 1965, p. 34—45

7. Ishimaru A. Theory of Unequally—Spaced Arrays IRE Transactions. v. AP—10, № 6, 1962, p. 691—702.

8. A. A. Kuz'min, V. M. Golovachev. Formation of the radiation pattern of arc antennas. "Antennas." Issue 5, 1969.

9. Ishimaru A., Bernard G. Tables of the Anger and Lommel—Weber functions. University of Washington Press, Seattle, Wash, 1962.

10. G. N. Watson. Theory of Bessel Functions, sections I, II. M., Pub. of foreign literature, M., 1949.

Received
4/IV/69.
Revised
1/XII/69.

EN

DAT